INTERNATIONAL ATOMIC ENERGY AGENCY
UNITED NATIONS EDUCATIONAL, SCIENTIFIC AND CULTURAL ORGANIZATION
INTERNATIONAL CENTRE FOR THEORETICAL PHYSICS
I.C.T.P., P.O. BOX 586, 34100 TRIESTE, ITALY, CABLE: CENTRATOM TRIESTE

UNITED NATIONS INDUSTRIAL DEVELOPMENT ORGANIZATION

INTERNATIONAL CENTRE FOR SCIENCE AND HIGH TECHNOLOGY
c/o INTERNATIONAL CENTRE FOR THEORETICAL PHYSICS 34100 TRIESTE (ITALY) VIA GRIGNANO, 9 (ADRIATICO PALACE) P.O. BOX 586 TELEPHONE [illegible]

SMR/543 - 15

EXPERIMENTAL WORKSHOP ON
HIGH TEMPERATURE SUPERCONDUCTORS AND RELATED MATERIALS
(BASIC ACTIVITIES)

(11 February - 1 March 1991)

---

" Radiation Effects on High Temperature Superconductors "

presented by:

WANG Guang-hou
Nanjing University
Department of Physics
Nanjing
P.R. China

---

# RADIATION EFFECTS ON HIGH TEMPERATURE SUPERCONDUCTOR

1. Purposes
   (1) Superconducting magnets and materials for future acceleractors and fusion reactors
   (2) Superconducting devicos by ion implantation and irradiation
   (3) Modification of superconductivities Jc, Tc, Hc
   (4) Stability of superconducting devices under irradiation for "High Techniques"
2. Experimentals
   (1) Materials:
      YBaCuO bulk
      YBaCuO / $SrTiO_3$, YSZ, Si substrates
   (2) particle beams
      Proton: 200 keV, 150keV, 50keV
      Electron: 8 MeV, 400keV

(3) Measurements

Electric measurement. $T_c$

X-ray diffraction

SEM. IR, Auger electron spectrum

High resolution transmission electron Microscope (HREM)

3. Computer simulation

(1) Range. Range distribution

Energy loss

Damage distribution

(2) Defects produced in YBaCuO

| Ion | Energy | Collision No. | Number of vacancy |
|---|---|---|---|
| $H^+$ | 350keV | 38.8 | 9.5 |
| O | 1MeV | 335 | 1068 |
| As | 1MeV | 532.7 | 7075.2 |

(3) Irradiation doses for certain vacancies produced

$10^{18}\ As^+/cm^2 \rightarrow 10^{21}\ O^+/cm^2 \rightarrow 10^{15} H^+/cm^2$

(4) Relation between Resistivity, Density of average defect energy $F_D$ and dose $\phi$:

$R = R_0 \exp(F_D \phi / 4)$

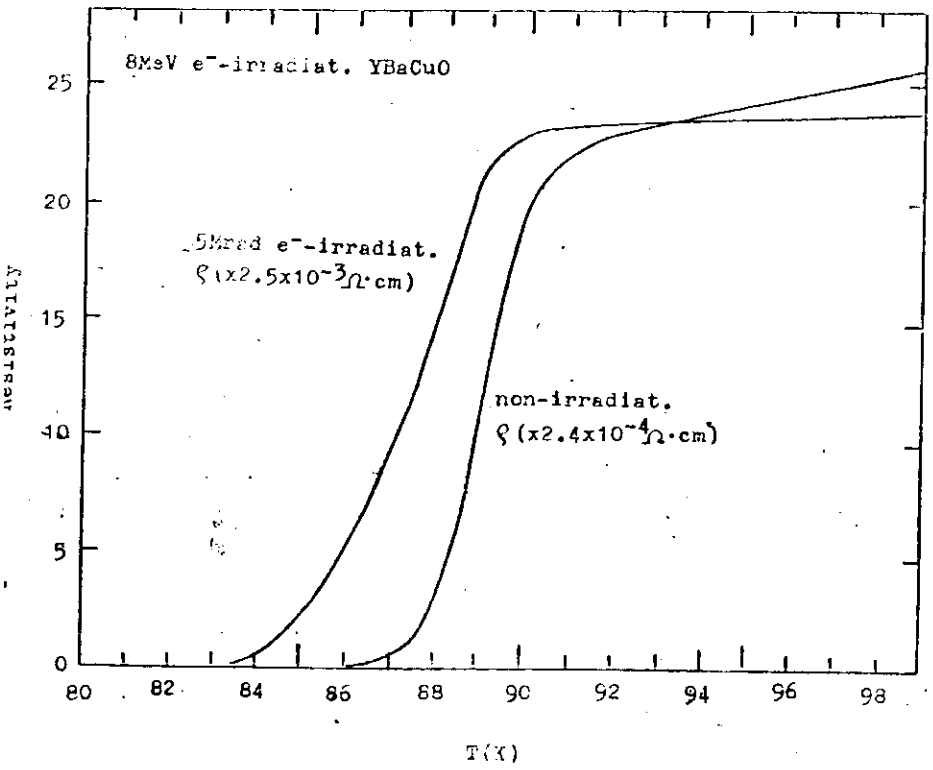

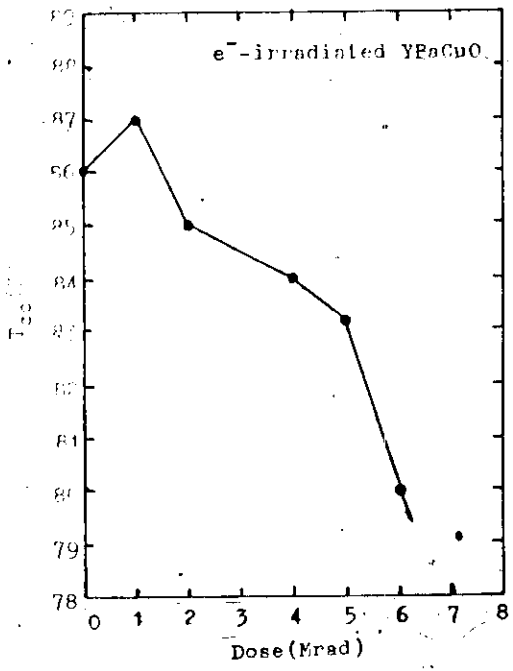
e⁻-irradiated YBaCuO
Dose(Mrad)
0
1
2
3
4
5
6
7
8
78
79
81
87



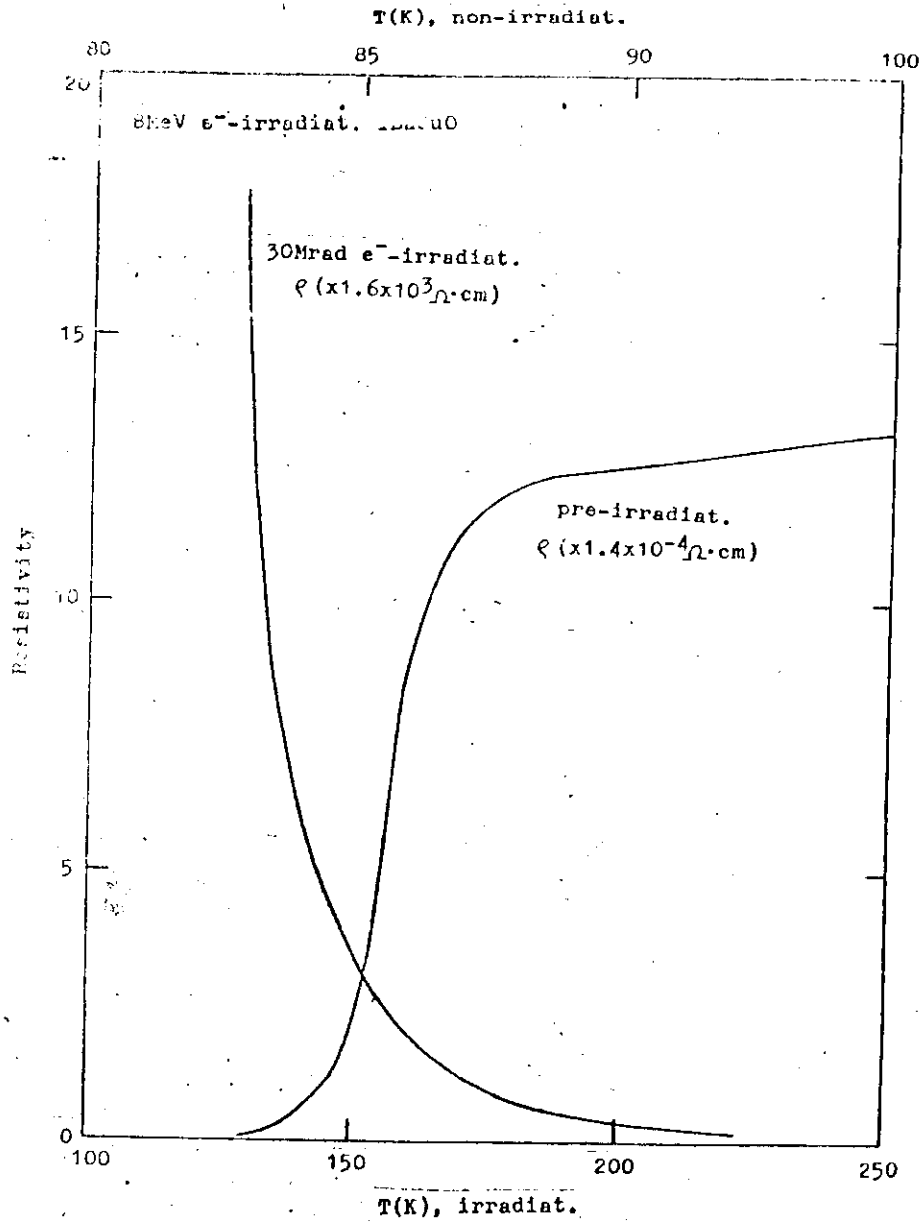
T(K), non-irradiat.
80
85
90
100
8MeV e⁻-irradiat.
30Mrad e⁻-irradiat.
ρ (x1.6x10³Ω·cm)
pre-irradiat.
ρ (x1.4x10⁻⁴Ω·cm)
Resistivity
0
5
10
15
20
100
150
200
250
T(K), irradiat.

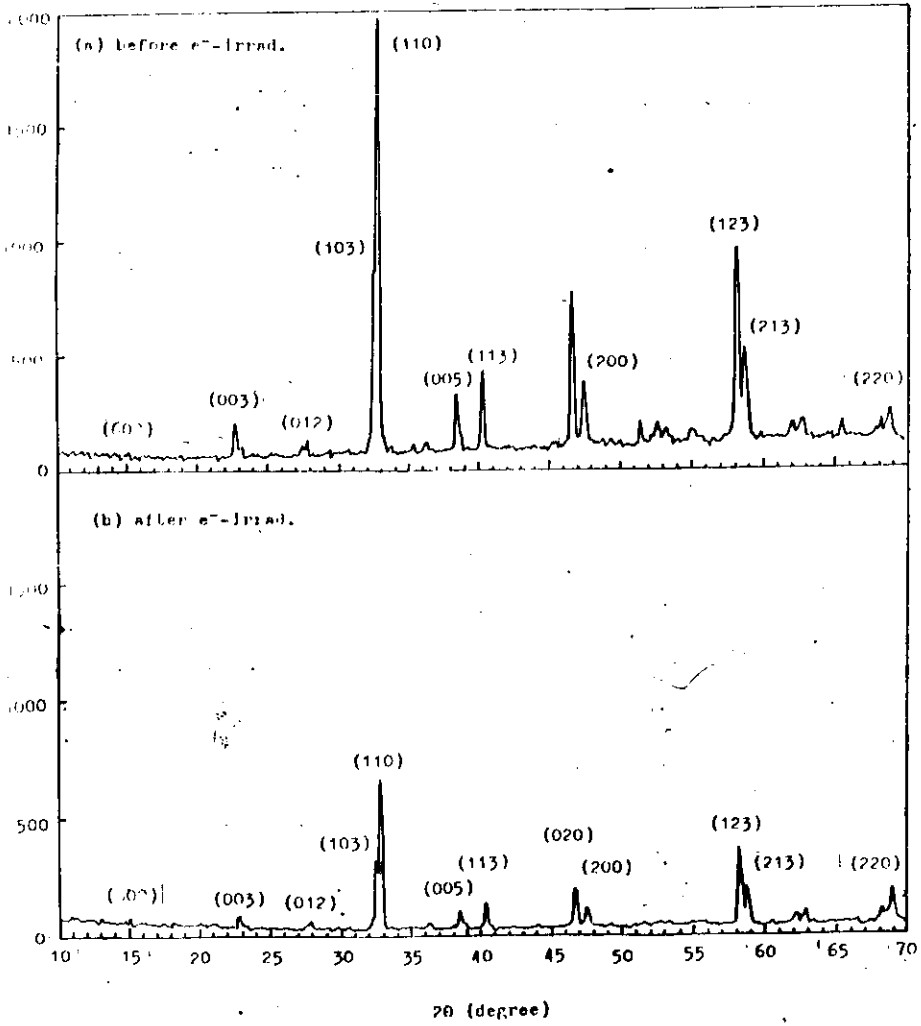




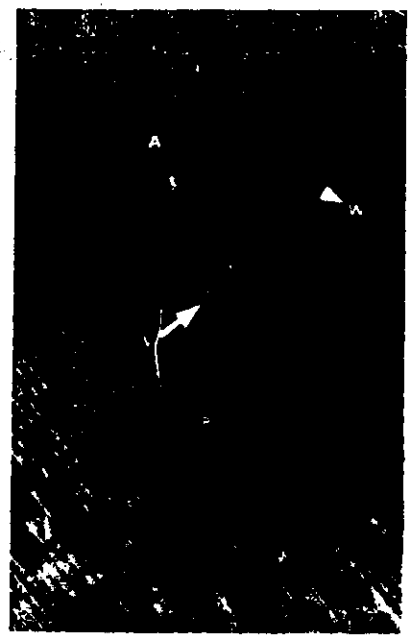


Fig. 6. High resolution electron microscope image of YBaCuO powder specimen with 156° angle of A and B. 1 cm corresponds to 5 nm.

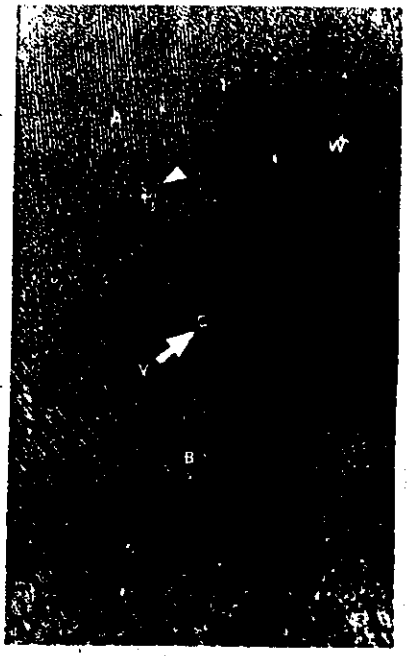


Fig. 7. High resolution electron microscope image of the specimen shows 146° angle of A and B in the same area after the 400 keV electron irradiation of $10^{20}$ $e^-/cm^2$ fluence. 1 cm corresponds to 5 nm.

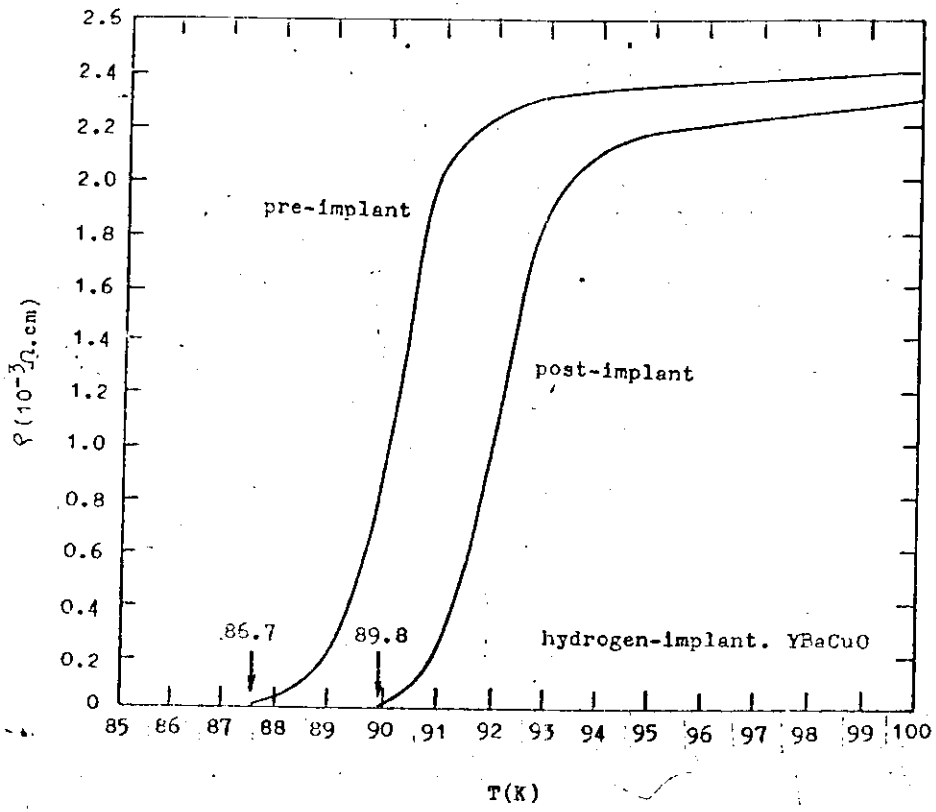
pre-implant
post-implant
86.7
89.8
hydrogen-implant. YBaCuO
ρ(10⁻³Ω.cm)
T(K)



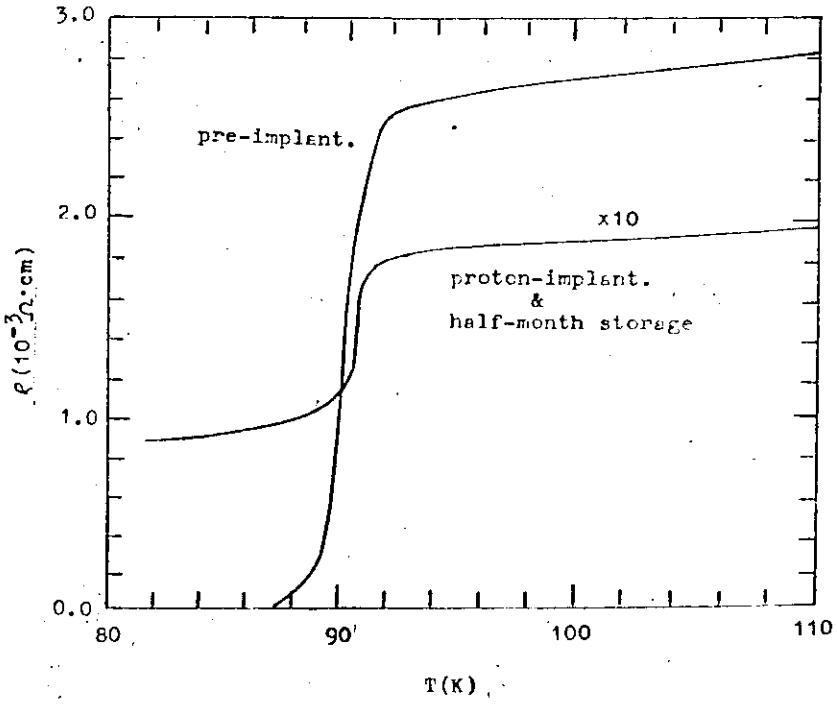
pre-implant.
x10
proton-implant.
&
half-month storage
ρ(10⁻³Ω.cm)
T(K)

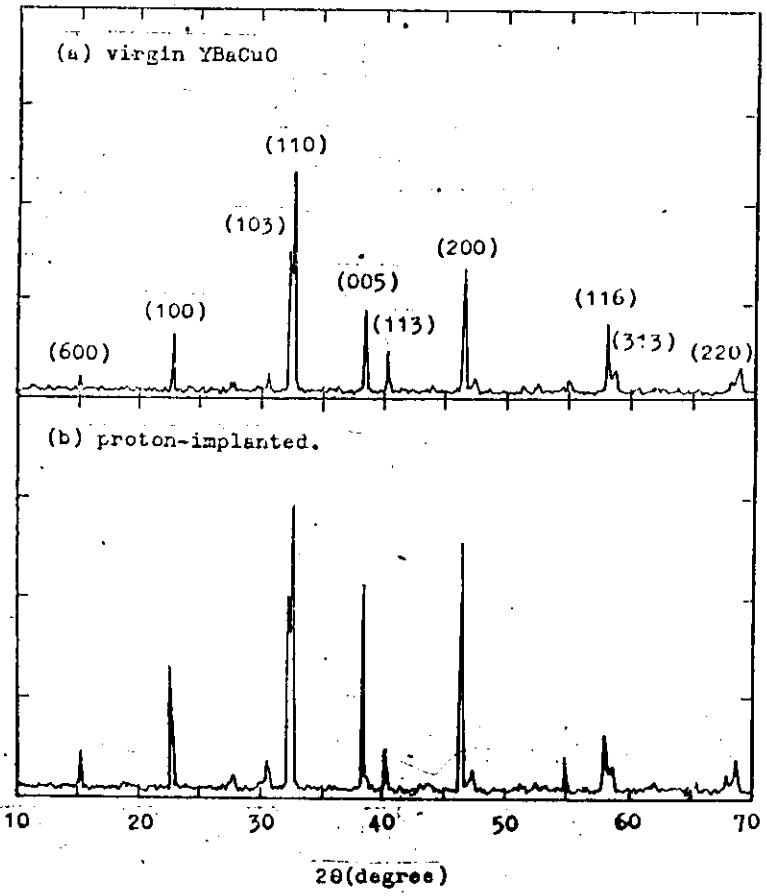
(a) virgin YBaCuO
(110)
(103)
(200)
(005)
(100)
(113)
(116)
(313)
(600)
(220)
(b) proton-implanted.
10
20
30
40
50
60
70
2θ(degree)

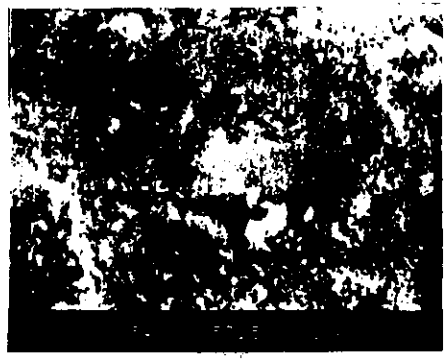

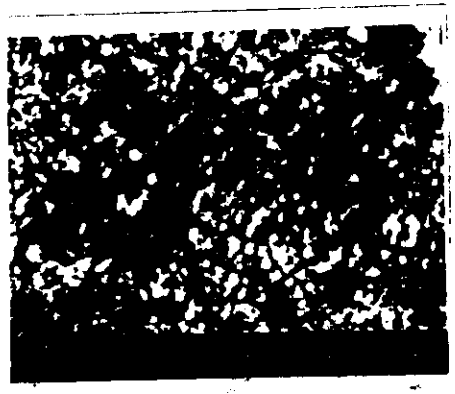

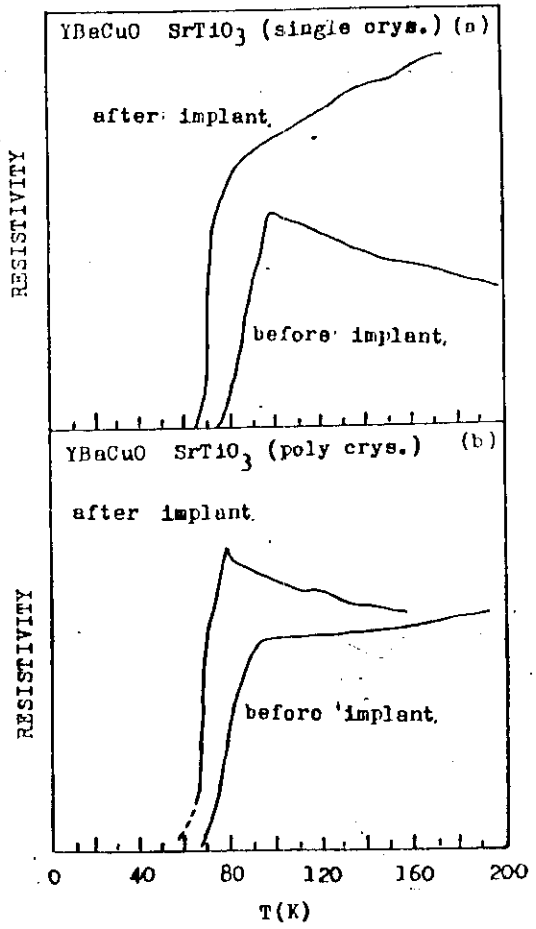
YBaCuO SrTiO3 (single crys.) (a)
after implant.
before implant.
RESISTIVITY
YBaCuO SrTiO3 (poly crys.) (b)
after implant.
before implant.
RESISTIVITY
0
40
80
120
160
200
T(K)



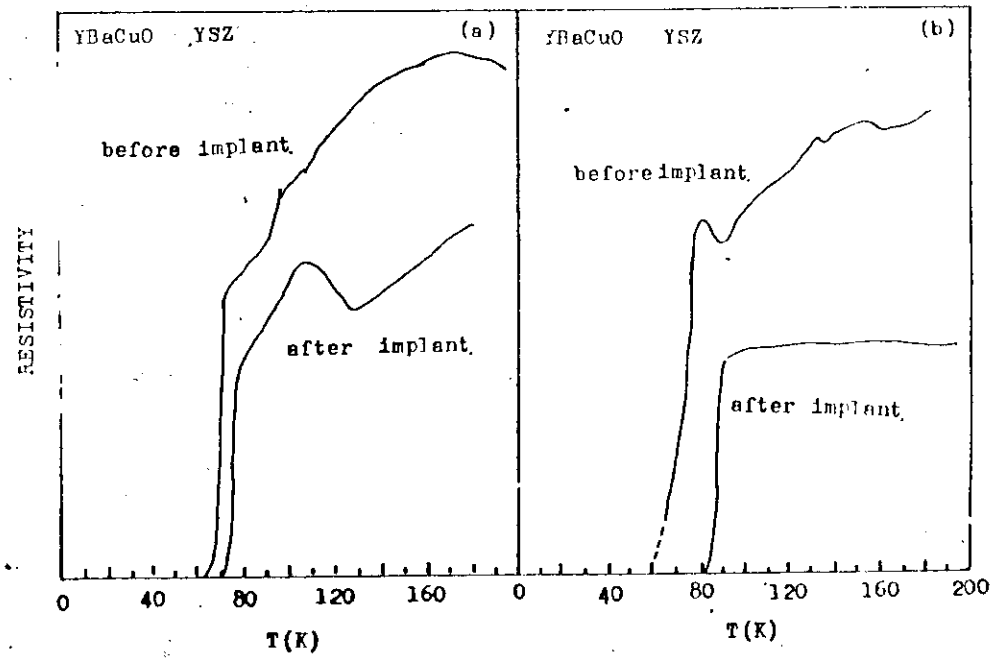
YBaCuO YSZ
(a)
before implant.
after implant.
RESISTIVITY
YBaCuO YSZ
(b)
before implant.
after implant.
0
40
80
120
160
200
T(K)

Table 1 Superconductivity of YBaCuO films with different substraten before and after proton implantation

| sample No. | Substrates | zero resistance temperature $T_{oo}$(K) | | Electric properties above the transition temperature | |
|---|---|---|---|---|---|
| | | virgin | implant | virgin | implant |
| 1 | Single Cryst. $SrTiO_3$ | 72.0 | 65.0 | semiconducting | metal |
| 2 | Poly Cryst. $SrTiO_3$ | 64.0 | below 60 ~ 50* | metal | semiconducting |
| 3 | Single Cryst. YSZ | 63.9 | 73.2 | metal | metal with a dip at 124K |
| 4 | Single Cryst. YSZ | below 60 ~55* | 78.0 | metal | metal |

* These values are obtained from the extrapolation due to the limitation of the measurement range.

5. Single cryst YBaCuO/YSZ — <60k, ~50K — 80 k — metal and higher normal resistance — metal



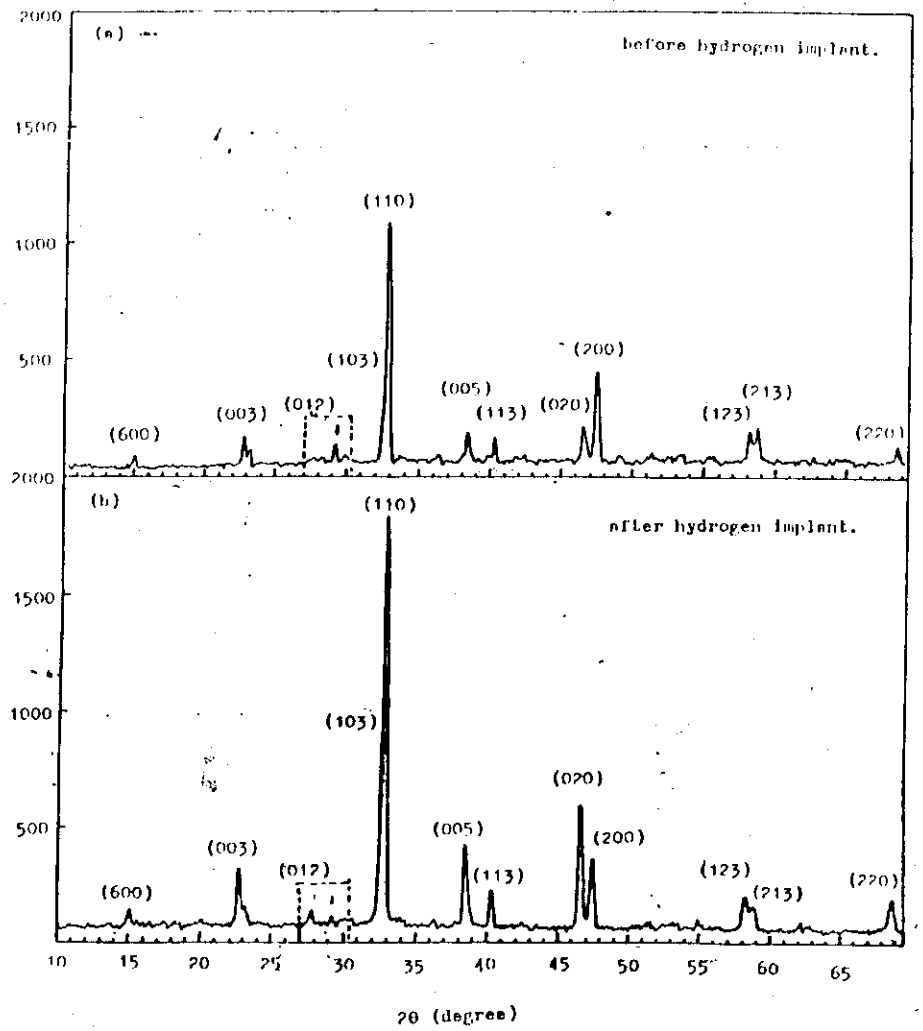

# X-ray diffraction Analysis

① Conversion from the tetragonal to orthorhombic phases.

Orthorhombic: $b \neq a = c/3$, peak (100) and (003) overlap but peak (100) separated with (010)

Tetragonal: $b = a \neq c/3$ peak (100) and (010) overlap but (100) separated with (003)

Therefore,

$$\left.\frac{I(003+100)}{I(010)}\right|_{ortho} > \left.\frac{I(003+100)}{I(010)}\right|_{tetra}$$

Also for planes (006) and (020), (116) and (213), etc.

| Ratio of Intensities | Before $H^+$-impl. | After $H^+$-impl. |
|---|---|---|
| $\frac{I(006+200)}{I(020)}$ | 0.315 | 1.63 |
| $\frac{I(116+213)}{I(123)}$ | 0.896 | 1.63 |
| $\frac{I(003+100)}{I(010)}$ | 1.360 | 1.543 |

Ratios increases indicate that the conversion from tetra- To ortho. phases



Table 3 Comparison of relative intensities for three pairs of crystal planes of YBaCuO films before and after implantation

| crystal planes | before | after |
|---|---|---|
| (012) and (102) | 6.0: 7.0 | 4.9: 3.5 |
| (020) and (200) | 13.8:43.9 | 32.4:19.9 |
| (123) and (213) | 14.5:16.2 | 12.2: 8.6 |

Table 4 Variation of c axes for three crystal planes of the YBaCuO film before and after proton implantation

| planes | before | after |
|---|---|---|
| 002 | 11.638 | 11.590 |
| 003 | 11.661 | 11.610 |
| 005 | 11.670 | 11.645 |

② Shortening of c-axis

For the planes with larger c index the distance d is obviously shortened after impl. while d does not change much for those with larger a and b indexes. The c axes of three YBCO crystal planes (002) (003) (005) are all shortened, the average value is decreased from 11.656 Å to 11.615 Å.

③ Decrease of non superconducting phase

$Y_2BaCuO_5$ phase characterized by $2\theta = 29.3°$, with ortho. nor tetra. decreased. while (102), (110) (005) (200) are enhanced.

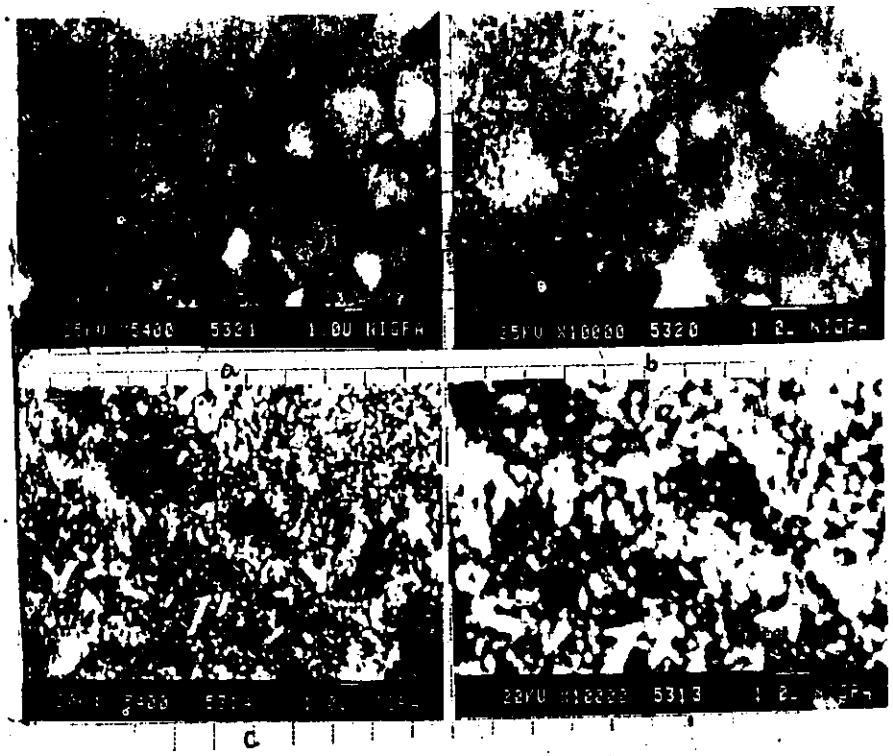




Scanning Electron Microscope

Magnification of 10,000 in the case of 20 kV.

① Finer crystal grains and smaller grains size

Before proton-irrad. disk-like 2 – 5 μm in diameter

After proton-irrad. bar-typed 0.2 μm in dia. and a length of ~1.5 μm

Proton bombardment makes crystal grains in YBCO film finer and more regular

② The density of crystal grains is increased by two orders of magnitude

From $10^6$ cm$^{-2}$ to $10^8$ grains cm$^{-2}$

③ The bar-typed grains in the implanted film have a preferential orientation perpendicular to the substrate surfaces, and parallel to each other.

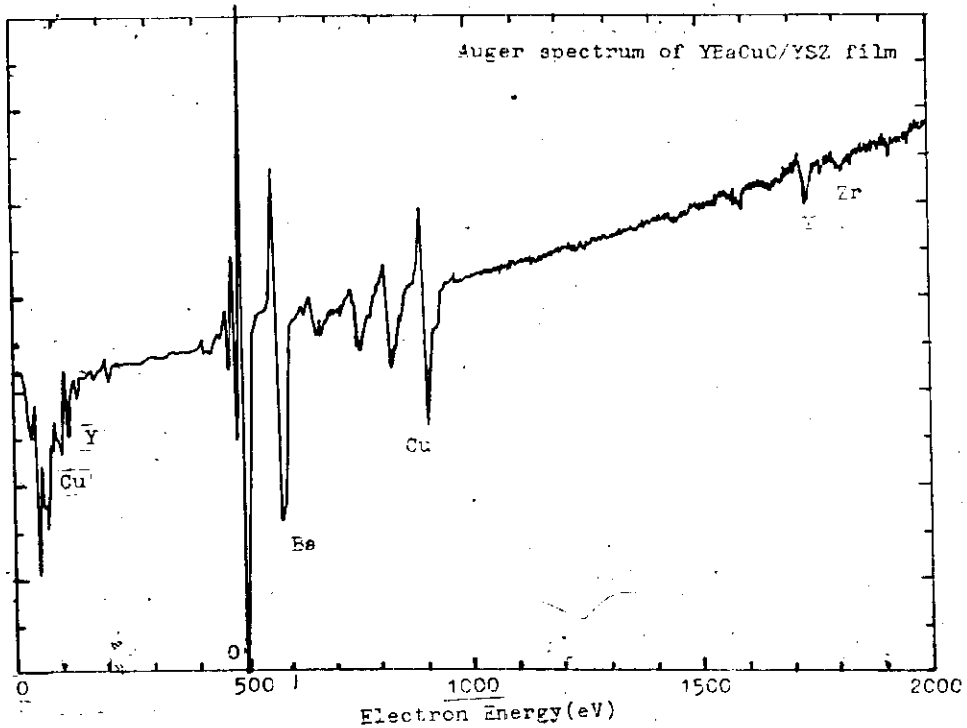
Auger spectrum of YBaCuO/YSZ film
Y
Cu
Ba
Cu
Zr
O
0
500
1000
1500
2000
Electron Energy(eV)

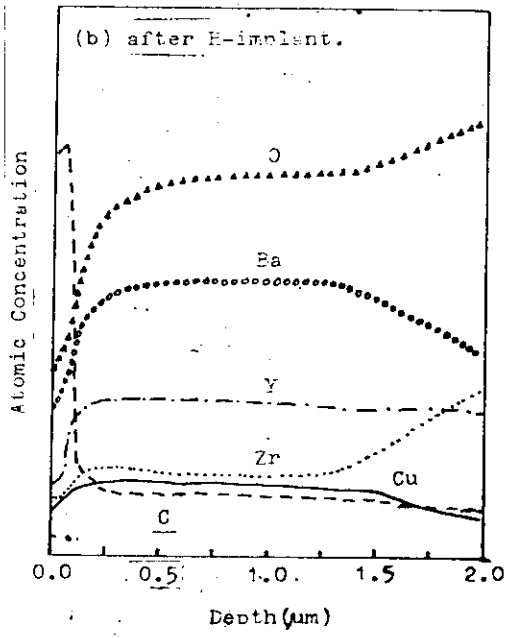
(b) after B-implant.
Atomic Concentration
O
Ba
Y
Zr
Cu
C
0.0
0.5
1.0
1.5
2.0
Depth(μm)

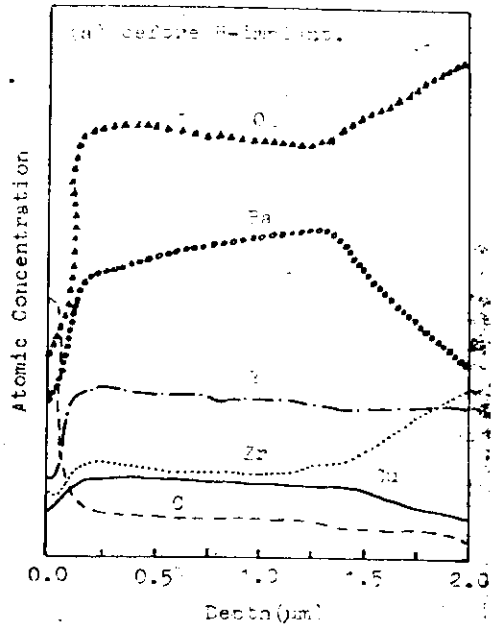
Atomic Concentration
O
Ba
Zr
0.0
0.5
1.0
1.5
2.0
Depth(μm)

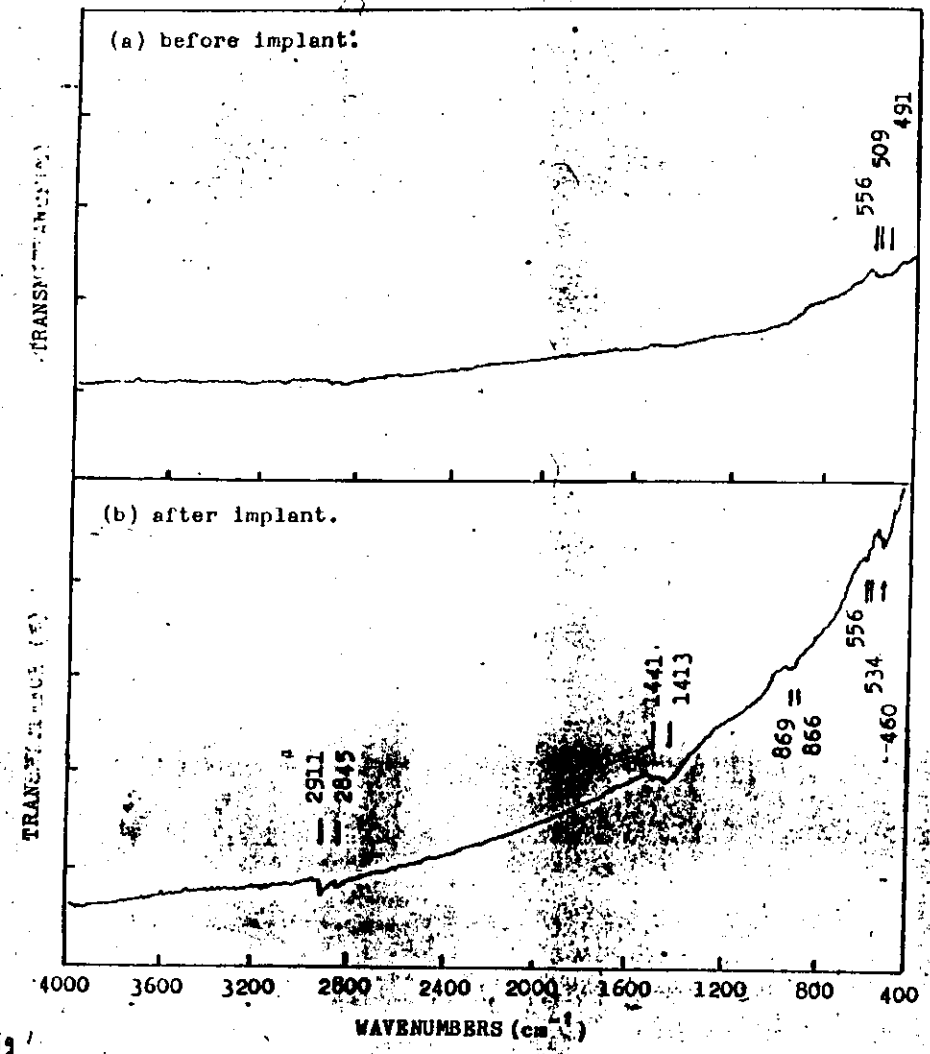


Fig 1



## IR spectra

(1) No H-O bond exists (1000 – 4000 $cm^{-1}$)

(2) Cu – O bond

Before 491, 509, 556 band vibration

After 460, 534, 556

(3) New bands in the implanted sample

1413 } due to Cu-H bond-stretching mode
1441 }

Hydrogen shift parallel to Cu-H bond

866 } come from Cu-H banding mode
869 }

Hydrogen shift vertical to Cu-H bond

(4) Line splitting and $H_I$, $H_{II}$ position

Symmetrical Consideration:

{866} and {869}: H near Cu(1) → $H_I$

{1413} and {1441}: H near Cu(2) → $H_{II}$

{2845} {2911} high order vibration modes

(5) Integal intensity of Cu-H stretching mode gives total number of ions for Cu-H bond.

Coordination number in IR polarization

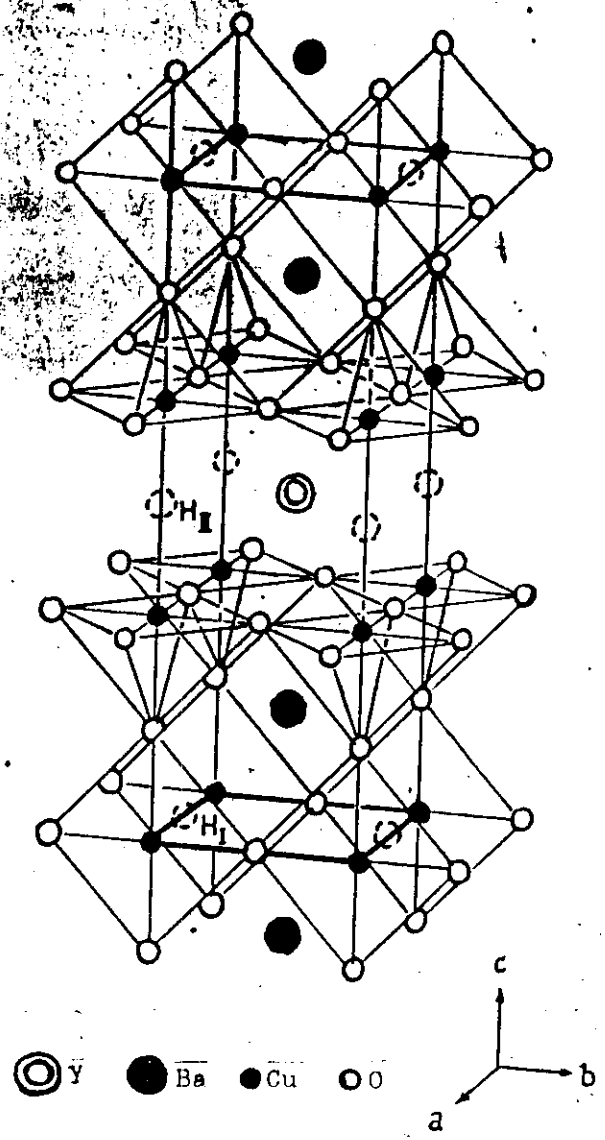




# RADIATION EFFECTS OF ELECTRONS AND PROTONS ON THE CERAMIC OXIDE SUPERCONDUCTOR YBaCuO

Guang-hou WANG, Jun CHEN, Guo-qiang PANG and Chen-lin LOU
*Department of Physics, Nanjing University, Nanjing, PR China*

Received 15 March 1988; accepted for publication 17 April 1988
Communicated by D. Bloch

The irradiation of the high $T_c$ superconducting material YBaCuO has been carried out by using 200 keV proton and 400 keV and 8 MeV electron beams. The temperature of zero resistance increases from 86.7 to 89.8 K with proton implantation while 8 MeV electron irradiation reduces the zero resistance temperature by 3 K with an irradiation dose of $2.25\times10^{17}$ e$^-$/cm$^2$. However, with an irradiation dose of $1.35\times10^{15}$ e$^-$/cm$^2$ the 8 MeV electron beam can make the superconductor become insulating. The in situ examination of a high resolution transmission electron microscope has proved that the amorphous region in the system has ordered arrangement whereas the crystalline region turns disordered under 400 keV electron irradiation with very high doses up to $10^{20}$ e$^-$/cm$^2$. The experiments demonstrate that proton and electron irradiations exhibit quite different effects both in its structure and property.

## 1. Introduction

There are three main reasons which have led to the study of irradiation effects in superconductors: (1) In order to select suitable superconducting material for magnets used in accelerators and possibly in fusion reactors one has to know the influence of radiation damage on $I_c$, $H_c$ and $T_c$. (2) The question as to whether irradiation or ion-implantation can provide more effective pinning centers than can be obtained by conventional techniques needs to be clear for fabrication of superconducting devices. (3) The stability of the superconducting devices under irradiation is an important factor in their application to "high techniques". Therefore, there has been considerable interest in the effects of irradiation of superconductors since 1960 and many studies have been concerned with the influence of radiation damage on the superconducting critical current and critical field at the conventional low $T_c$ superconducting materials. Irradiations were performed using neutrons, protons, deuterons and alpha-particles and striking effects were reported for the critical current density. However, little influence of radiation damage on the superconducting transition temperature has been observed [1].

Bednorz and Müller reported in 1986 a superconducting transition temperature, $T_c$, above 30 K for ceramic oxides [2]. This value was soon raised up to 90 K in the YBaCuO system prepared by many groups around the world [3,4]. High upper critical fields [5], $B_{c2}$, and the capability of carrying high critical current densities [6], $J_c$, offer the possibility of application of this new superconducting material at the liquid nitrogen temperature. One prospect of these exciting materials is a high current application in magnet technology, e.g. in magnetic plasma confinement for fusion reactors or in beam guiding magnets for high energy physics. In these systems the superconductor will be exposed to radiation with high fluence particles. Therefore, it is necessary to investigate the changes of the superconducting properties with irradiation damage. Very recently, Küpfer et al. [7] used fast neutrons to irradiate $YBa_2Cu_3O_7$ up to a fluence of $10^{19}$ n/cm$^2$ ($E\geq1$ MeV), and obtained that the $T_c$ degradation with fluence was slightly less than in $PbMo_6S_8$, but larger than in A15 compounds. In this paper we report radiation effects of a YBaCuO superconducting sample by energetic electrons and protons in quite different ways.

0375-9601/88/$ 03.50 © Elsevier Science Publishers B.V.
(North-Holland Physics Publishing Division)

## 2. Experimental

The samples were made by using the common sintering technique, i.e. the oxide method, first mixing $BaCo_3$, $Y_2O_3$ and CuO, grinding, pressing into pellets again, sintering at 940–970°C in flowing $O_2$ for 12 hours, finally cooling to 200°C in $O_2$ before removing from the furnace [8]. From X-ray diffraction investigation the material was characterized to be chemically homogeneous and single phased.

The 200 keV proton irradiation was performed by the ion implantor (Chang Sha) with a fluence of $10^{15}$ p/cm$^2$ under vacuum condition ($10^{-5}$ Torr working pressure). An 8 MeV electron beam was used to irradiate the samples with three different fluences of $2.25\times10^{14}$, $6.75\times10^{14}$ and $1.35\times10^{15}$ e$^-$/cm$^2$ from the 20 MeV electron linear accelerator designed and manufactured by the Nanjing University. The resistivity of the samples before and after implantation was measured by the standard four-probe method with temperature change from liquid nitrogen to room temperature.

The in situ structural observation of the 400 keV electron-irradiated samples was done by a JEM-4000EX electron microscope in the following two ways. Some samples were thinned by ion-milling and called type 1, while the others, first crushed into small particles and then sprinkled onto holey carbon amorphous films were called type 2.

## 3. Results and analysis

Fig. 1 shows the resistivity versus temperature curves of a YBaCuO superconducting sample before and after proton implantation, which indicates that not only does the sample keep superconductivity but its transition temperature becomes higher after the irradiation, i.e., the zero resistance transition temperature is raised from 86.7 to 89.8 K. In order to investigate the radiation effect of the superconducting stability both proton-irradiated and non-irradiated samples were stored at rather humid atmosphere for half a month, and then measured again. The surface of the non-irradiated sample was eroded and became insulated with a resistivity up to $10^4$ Ω cm, while the proton-modified sample kept well-conducting though its zero resistance temperature did

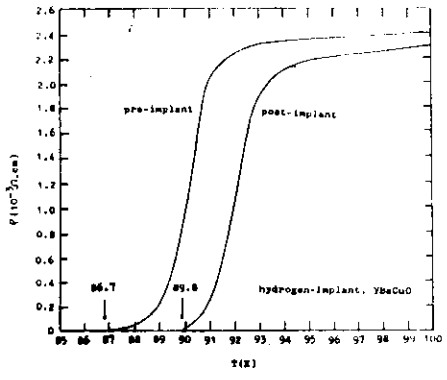


Fig. 1. Resistivity–temperature curves of YBaCuO superconductor before and after proton irradiation.

not appear within the range of measurement. Fig. 2 shows the $R$–$T$ curve of the implanted YBaCuO superconducting sample after half a month storage at atmospheric condition, in which the resistivity drops down obviously when the temperature approaches to critical one although it does not exhibit zero value. This demonstrates that the proton irradiation may also stabilize the ceramic oxide superconductor.

Under 8 MeV electron irradiation the zero resistance temperature of the superconductor is decreased from 86 to 83.2 K at a fluence of $2.25\times10^{14}$

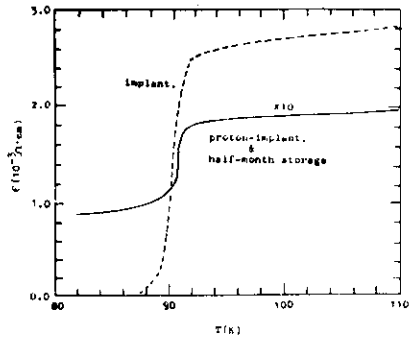


Fig. 2. Resistivity versus temperature of the proton-implanted superconducting sample with half a month storage in the atmosphere.





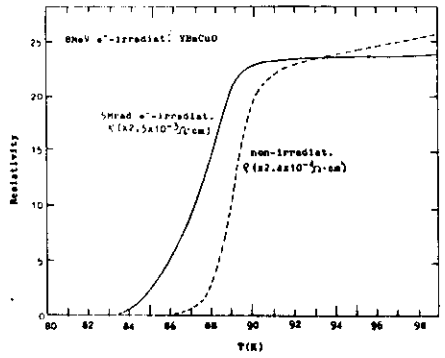


Fig. 3. $R$–$T$ curves for YBaCuO superconducting sample before and after 8 MeV electron irradiation with the fluence of $2.25\times10^{14}$ e$^-$/cm$^2$.

e$^-$/cm$^2$, shown in fig. 3. However, with irradiation doses of $6.75\times10^{14}$ and $1.35\times10^{15}$ e$^-$/cm$^2$ the superconducting samples become insulated. Fig. 4 presents the $R$–$T$ curves of the sample before and after $1.35\times10^{15}$ e$^-$/cm$^2$ electron irradiation. Therefore, the radiation effect of electrons on the YBaCuO superconductor is closely related to the irradiation dose.

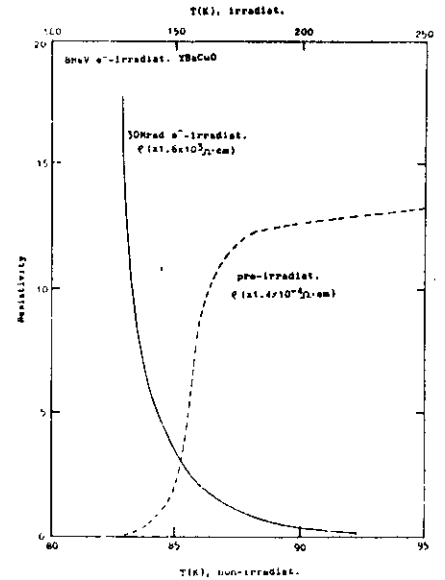


Fig. 4. $R$–$T$ curve of the YBaCuO superconductor after 8 MeV electron irradiation with the fluence of $1.35\times10^{15}$ e$^-$/cm$^2$.

X-ray diffraction spectra of the superconducting sample with and without proton irradiation are shown in fig. 5, in which the diffraction peaks that appeared before the irradiation still exist after irradiation. That is to say, the values of the primitive vectors $a$, $b$, $c$ of the crystallographic cell have not changed after the irradiation. However, we have found that the intensities of the peaks increase dramatically with proton implantation, and the relative intensities change quite a bit too. Table 1 lists the intensities and the relative intensities of the X-ray diffraction peaks for both irradiated and non-irradiated cases. The former point can be explained by considering that the irradiated sample is denser than the non-irradiated one, which means that the hydrogen implantation creates more microcrystal surfaces per unit area reflecting the X-rays, while the latter is related to the change of internal atomic structure of crystallographic cells. The different densities between the irradiated and the virgin samples have also been seen by scanning electron microscope where the implanted sample shows finer grains. Therefore, it is

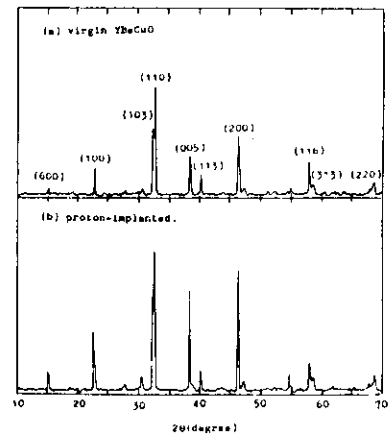


Fig. 5. X-ray diffraction spectra of YBaCuO superconductor before (a) and after (b) proton-implantation.

able 1
ntensities and relative intensities of X-ray diffraction peaks for roton-irradiated and non-irradiated YBaCuO sample. $I_n$: peak tensity for non-irradiated sample. $I_i$: peak intensity for irradied sample $I_m$: intensities of the peaks for $2\theta = 32.818$.

| $2\theta$ | $D$ | $(hkl)$ | $I_n$ | $I_n/I_m$ | $I_i$ | $I_i/I_m$ |
|---|---|---|---|---|---|---|
| 15.191 | 5.827 | 600 | 48 | 9.2 | 92 | 15.7 |
| 22.860 | 3.887 | 100 | 130 | 27.8 | 279 | 47.6 |
| 30.680 | 2.911 | | 49 | 10.5 | 77 | 13.1 |
| 32.514 | 2.752 | 103 | 272 | 58.2 | 381 | 65.2 |
| 32.818 | 2.727 | 110 | 467 | 100.0 | 586 | 100.0 |
| 38.572 | 2.332 | 005 | 190 | 40.7 | 434 | 74.1 |
| 46.362 | 2.232 | 113 | 99 | 21.2 | 101 | 17.2 |
| 46.694 | 1.943 | 200 | 270 | 57.8 | 520 | 88.7 |
| 58.242 | 1.582 | 116 | 161 | 34.5 | 134 | 22.9 |
| 58.806 | 1.568 | 313 | 57 | 12.7 | 67 | 11.4 |
| 68.845 | 1.362 | 220 | 66 | 14.1 | 78 | 13.3 |

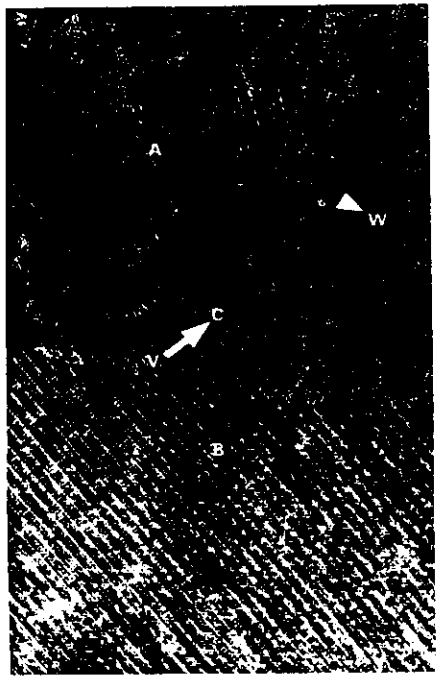


Fig. 6. High resolution electron microscope image of YBaCuO powder specimen with 156° angle of A and B. 1 cm corresponds to 5 nm.

conjectured that the proton implantation may raise the critical current density of superconductivity in the YBaCuO system because more surfaces of the crystallines are created by hydrogen interactions.

The high resolution electron microscope (HREM) observations confirm that three regions coexist in all YBaCuO superconducting samples: the crystalline or ordered region (OR); the amorphous or disordered region (DR) and the transition region between the two. Fig. 6 is the HREM image along the [010] zone obtained in a powder specimen. In the region marked A in the picture one can see dimly many one-dimensional lattice line-images extended deeply into the DR region. Such line-images are spaced with triple period, of about 11.7 Å. However, it is difficult

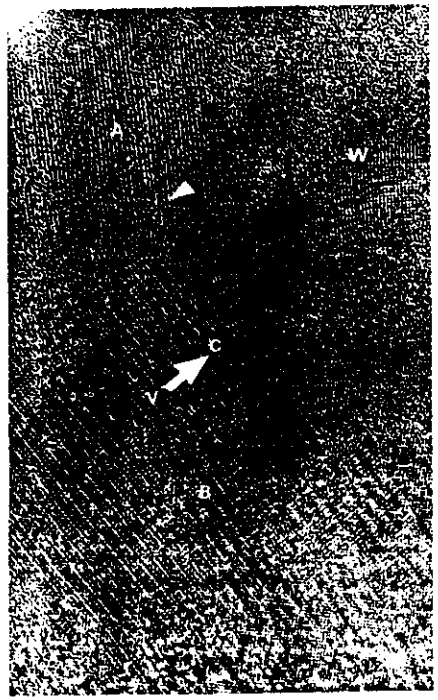


Fig. 7. High resolution electron microscope image of the specimen shows 146° angle of A and B in the same area after the 400 keV electron irradiation of $10^{26}$ e /cm$^2$ fluence. 1 cm corresponds to 5 nm.



to see ordered particles in the DR and TR region. The lower-right part of the picture is the OR region in which the two-dimensionally well imaged lattices can be seen clearly, shown by mark B. The two directions with triple period in the A and B region intersect by an angle of 156°. Fig. 7 shows a HREM image at the same area of the specimen after 400 keV electron bombardment with a dose of $3.6\times20^{26}$ e / cm$^2$. From figs. 6 and 7 we conclude:

(a) The angle between two [001] directions, which are just the directions of both triple period in A and B regions, changes from 156° (in fig. 6) to 146° (in fig. 7) after keeping on electron irradiation for about an hour.

(b) The electron irradiation may render the crystalline phase amorphous or disordered as shown at mark V in these pictures. In fig. 6 the V area is imaged well with two-dimensional lattices, we think that the bright spots may correspond to heavy metal atomic columns, while in fig. 7 some rather disordered structures appear on the same region.

(c) In the DR region local recrystallization may occur after nearly one hour of irradiation, as shown on the region indicated by W in fig. 7. The recrystalline particle size is about 10 nm.

## 4. Conclusion and discussion

From the above study we may draw the following conclusions:

(1) Ionizing radiation by energetic protons can improve the properties of YBaCuO superconducting material, for instance, to raise its transition temperature and stability. Microscopically the proton irradiation may fine the grains of the ceramic oxide superconductor so that the critical current density of the superconductor can be raised if its superconducting comes from the interfaces between the lattice grains.

(2) The high energy electron irradiation (8 MeV) degrades the transition temperature of the superconductor in general, and even makes YBaCuO material insulating with higher irradiation doses. However, this effect may be used as a tool to fabricate Josephson junctions directly on the superconducting sample when the electron beam is focused as a microbeam.

(3) At high dosage ($10^4$ A/cm$^2$) 400 keV electron irradiation causes structural changes within the ceramic superconducting sample along two opposite directions: one is the amorphorization of the crystalline phase and the other the recrystallization of the amorphous phase. In our in situ HREM experiments the disordering looks like the dissolution of thermally stable phase and the recrystallization like precipitation of phases not thermally stable.

On the other hand the proton irradiation can improve the superconductivity of the YBaCuO system though 200 keV protons can penetrate only micrometers in depth of the sample. At present it is hard to say whether the different radiation effects on the YBaCuO system by electrons and protons are due to the particle energies or due to the different interaction mechanism similar to that in polymers [9]. It is known that several complicated processes may occur in solids simultaneously under irradiation: such as precipitation of thermally stable phases, dissolution of thermally stable phases, disordering of ordered precipitates, production of radiation defects, as well as irreversible segregation and/or aggregation of solute to or away from dislocations and interfaces. The predominant process depends on the irradiation dose, dose rate and the energy of the particles, etc. Experiments with different incident energy and different dose as well as various kinds of measurements are under way in order to study further the above problems. Our present results demonstrate that different particles affect the properties of such a ceramic oxide superconductor in different ways.

## Acknowledgement

Acknowledgement is made to Professors D. Feng, C.D. Gong, P.H. Wu, X.X. Yao for their support of our work and our colleagues in the Electron Linear Accelerator for help with electron irradiation.

## References

[1] G.H. Wang and He Wuli Dongtai, Persp. Nucl. Phys. 4(3) (1987) 6.
[2] J.G. Bednorz and K.A. Müller, Z. Phys. B 64 (1986) 189.
[3] M.K. Wu, J.R. Ashburn, C.J. Torng, R.H. Hor, P.L. Meng, L. Gao, Z.J. Huang, Y.Q. Wang and C.W. Chu, Phys. Rev. Lett. 58 (1987) 908.

[4] Z.X. Zhao, L.Q. Chen, Q.S. Yang, Y.Z. Huang, G.H. Chen, R.M. Tang, G.R. Liu, C.G. Gui, L. Chen, L.H. Wang, S.Q. Guo, S.L. Li and J.Q. Bi, Kexue Tongbao 32 (1987) 661.
[5] T.P. Orlando, K.A. Delin, S. Foner, E.J. McNiff Jr., J.M. Tarascon, L.H. Greene, W.R. Mckinnon and G.W. Hull, Phys. Rev. B 35 (1987) 7249.
[6] P. Chaudhary, R.H. Koch, R.B. Laibowitz, T.R. McGuire and R.J. Gambino, Phys. Rev. Lett. 58 (1987) 2684.
[7] H. Küpfer, L. Apfelstedt, W. Schauer, R. Flükiger, R. Meier-Hirmer and H. Wühl, to be published in Z. Phys. B.
[8] M.K. Teng, D.X. Shen, L. Chen, C.Y. Yi and G.H. Wang, Phys. Lett. A 124 (1987) 363.
[9] G.H. Wang, X.J. Li, Y.Z. Zhu, Q.S. Liu, N.X. Hu, X.S. Gu and Q. Wang, Nucl. Intrum. Methods B 7/8 (1985) 497.





# MODIFICATION OF YBaCuO SUPERCONDUCTING FILMS BY HYDROGEN IMPLANTATION

Guang-hou WANG [1], Guo-giang PANG, Cheng-lin LUO
*Department of Physics, Nanjing University, Nanjing, PR China*

Sen-zu YANG, Yen LI, Zheng-ming JI and Zhi-jian SUN
*Department of Information Physics, Nanjing University, Nanjing, PR China*

Received 20 April 1988; accepted for publication 18 May 1988
Communicated by D. Bloch

The effects of hydrogen implantation into ceramic superconducting films have been studied. The superconductivity changed dramatically and is closely related to the substrates supporting the films. In the case of $SrTiO_3$ substrate the superconducting transition temperature, $T_{c0}$ (the zero resistance temperature), is reduced while it is greatly raised up with YSZ substrate after 150 keV $H^+$ implantation. X-ray diffraction investigation has proved that the microstructure of the YBaCuO film with YSZ substrate has been modified by shortening the *c*-axis. The infrared absorption spectra have shown that the emergence of new vibrational frequencies of 2911, 2845 as well as 1441 and 1413 $cm^{-1}$ representing the formation of Cu–H bonds at the different positions of the crystal cell may affect the superconductivity.

## 1. Introduction

In searching superconductivity with high $T_c$ values the materials showing structured instabilities exhibit the best results, such compounds or alloys with compositions close to the phase transition region or metastable compounds produced by non-equilibrium processes such as splat cooling, evaporation and sputtering. Ion implantation as nonequilibrium method is thought to be of interest in this respect because of its inherent possibility to increase solubility levels above thermal equilibrium values and to produce metastable alloys, as well as to compensate deviations from stoichiometry and to fill vacancies in sublattices of compounds which cannot correctly be formed by conventional techniques. An excellent example of the usefulness of ion implantation was demonstrated by Bückel and Stritzker [1], who succeeded in preparing superconducting Pd–H alloys by means of H implantation at liquid helium temperature: the $T_c$ was increased with increasing fluence of H ions and the maximum $T_c$ value of 9 K estimated for a H/Pd ratio of about 1, which is not easily obtained by other techniques. This work was extended to the H-implanted Pd–noble metal system [2], and the highest $T_c$ of 16.7 K was obtained in the Pd–Cu–H system [3]. In spite of these efforts, $T_c$ did not exceed 23.2 K of $Nb_3Ge$.

In 1986, Bednorz and Müller [4] reported compound oxides with a higher superconducting transition temperature, $T_c = 35$ K. Subsequently, the $T_c$ values were raised to 90 K in the ceramic oxide $YBa_2Cu_3O_x$ [5]. This offered the possibility of operating superconducting devices at liquid nitrogen temperatures. A significant step in this direction was the preparation of superconducting thin films with composition close to $YBa_2Cu_3O_x$ by Laibowitz et al. [6], having complete transition temperatures above 85 K. These thin films were then used to fabricate and operate at 68 K a weak link dc SQUID by patterning the films using radiation damage induced by ion implantation. In this paper, we shall report modification of superconductivity in YBaCuO films by

[1] Also at the Laboratory of Solid-State Microstructures, Nanjing University, Nanjing, PR China.

0375-9601/88/$ 03.50 © Elsevier Science Publishers B.V.
(North-Holland Physics Publishing Division)

hydrogen ion implantation. A great enhancement of the transition temperature in the ceramic superconducting films supported by yttrium-doped zirconium oxide substrate has been observed.

## 2. Experimental

Films of nominal composition $YBa_2Cu_3O_x$ were prepared by rf magnetically controlled sputtering from the corresponding bulk material of superconductivity and deposited onto three different substrates respectively: single- and poly-crystal $SrTiO_3$ and the crystal Y-doped $ZrO_2$ (YSZ), which were held at 400°C. They were subsequently annealed in 1 atm. $O_2$ in an oven set to 910°C. After annealing, the thickness of the film used in this study was about 1 μm. Chemical analysis confirmed that their mean compositions were near the "123" composition.

The 150 keV proton irradiation was carried out by the IM-200M Ion Implantor (Japan) with a fluence of $1.6\times10^{15}$ p/cm$^2$ under vacuum condition ($\sim10^{-5}$ Torr working pressure).

The resistivity of the sample before and after implantation was measured by the standard four probe method with temperature change from below liquid temperature (62 K) to room temperature. Structural studies of the superconducting films before and after proton implantation were analyzed by FT infrared spectroscopy (Nicolet Analytical Instruments 170-SX) and X-ray diffraction by using CuKα monochromatic radiation with a wavelength of 1.5418 Å, and a scanning speed of 0.5° and a counting rate of 500 cps. Both proton irradiation and the structural measurements were done at 295 K (room temperature) and the temperature variations during the measurements were less than ±1.0 K.

## 3. Superconductivity

Figs. 1 and 2 show the resistivity versus temperature curves of several YBaCuO superconducting films with different substrates before and after proton implantation. The materials of these substrates are single-crystal $SrTiO_3$ (fig. 1a), polycrystal $SrTiO_3$ (fig. 1b) and single-crystal YSZ (yttrium-doped zirconium oxide) (figs. 2a and 2b). The two curves

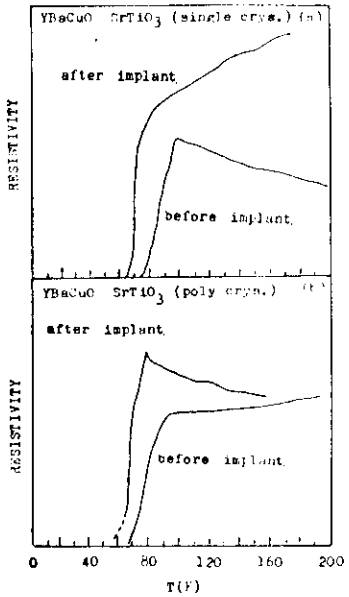


Fig. 1. Resistivity–temperature curves of YBaCuO superconducting films with different substrates: (a) single-crystal $SrTiO_3$; (b) polycrystal $SrTiO_3$.

in figs. 1b and 2b with the dotted part on the low-temperature side do not show the zero resistance temperature ($T_{c0}$) due to the limitation of the measurement range (62 K). Table 1 presents the results of RT measurements.

The following information can be obtained from figs. 1, 2 and table 1:

(1) In the case of substrate $SrTiO_3$, either single- or poly-crystal, the zero resistance transition temperature of YBaCuO superconducting films decreases after proton irradiation, but their electric properties above the transition temperature changed in a different way: in the former, from semiconductor to metal (see fig. 1a), while in the latter from metal to semiconductor (see fig. 1b).

(2) The superconducting YBaCuO films supported by single-crystal YSZ substrate show a much higher $T_{c0}$ after hydrogen implantation. For sample 3, $T_{c0}$ raises from 63.9 to 73.2 K and for sample 4





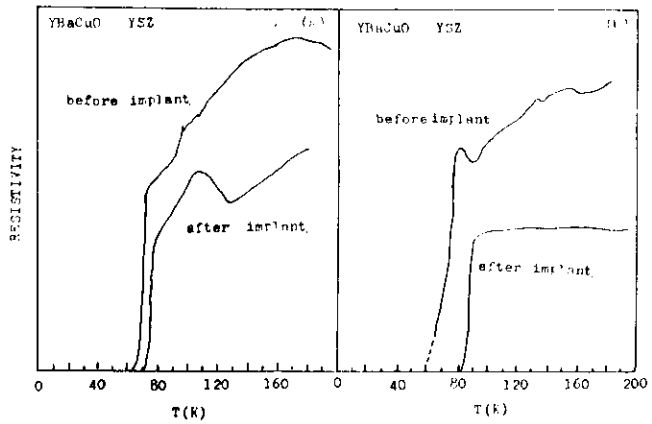


Fig. 2. Resistivity–temperature curves of YBaCuO superconducting films supported by zirconium oxide doped with yttrium (YSZ).

it reaches 78.0 K from ~55 K to 78 K (within our measurement range it cannot reach the zero resistance before implantation but it may have a zero resistance temperature of 55 K from extrapolation). Both samples 3 and 4 have better electric characteristics above the transition temperature after hydrogen implantation.

These indicate that (a) hydrogen implantation can modify superconductivity of YBaCuO films and (b) this modification is closely related to the structure and properties of the supporting materials.

## 4. Structural analysis

Radiation can induce structural changes in the ceramic oxide superconductor YBaCuO [7], and the change of these films can be studied by X-ray diffraction and infrared absorption. X-ray diffraction spectra of YSZ-supported YBaCuO film before and after hydrogen implantation are shown in fig. 3, in which the diffraction peaks that appeared before implantation still exist after implantation. That is to say, the values of the primitive vectors of the crystallo-

Table 1
Superconductivity of YBaCuO films with different substrates before and after proton implantation.

| Sample | Substrates | Zero resistance temperature $T_{c0}$ (K) | | Electric properties above the transition temperature | |
|---|---|---|---|---|---|
| | | virgin | implant | virgin | implant |
| 1 | single-crystal $SrTiO_3$ | 72.0 | 65.0 | semiconducting | metal |
| 2 | polycrystal $SrTiO_3$ | 64.0 | < 60<br>~ 50 [a] | metal | semiconducting |
| 3 | single-crystal YSZ | 63.9 | 73.2 | metal | metal with a dip at 124 K |
| 4 | single-crystal YSZ | < 60<br>~ 55 [a] | 78.0 | metal | metal |

[a] These values are obtained from the extrapolation due to the limitation of the measurement range.

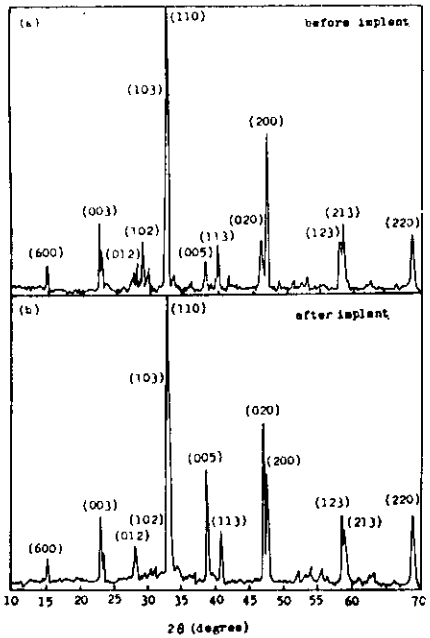


Fig. 3. X-ray diffraction spectra of YBaCuO film with YSZ substrate: (a) before hydrogen implantation, (b) after hydrogen implantation.

graphic cell do not change much after the proton irradiation. This has been proved by scanning electron microscope in which the surface morphology of the film does not show obvious change with or without irradiation. However, the relative intensities of X-ray diffraction peaks change dramatically before and after hydrogen implantation, especially for the planes (102), (005), (113), (020), (200), (123) and (213), etc. Table 2 lists the relative intensities of X-ray diffraction and distances $d$ between the main crystal planes of the superconducting film before and after proton implantation. Table 3 gives a comparison of the relative intensities of a few sets of the crystal planes and table 4 presents the changes of $c$-axes for the planes (002), (003) and (005) with the proton irradiation. Several fearures are observed:

First, both the virgin and implant films with YSZ substrate have orthophase structure and a superconducting phase.

Second, planes (020) and (200), (213) and (123), (102) and (012) are pairs of the crystal planes equal for $a$ and $b$ directions, the plane with bigger index $a$ has larger relative intensity for the virgin sample, for instance, the plane (102) has an intensity of 7.0 while (012) has 6.0; it is just opposite after hydrogen implantation that the plane with bigger index $b$ has larger intensity, for example, (102) plane has 3.5 and (012) plane has 4.9. Table 3 gives a comparison for other pairs of planes as (020) and (200), (123) and (213). This demonstrates that proton implantation has induced a microstructural change of the crystal lattice in the YBaCuO superconducting film.

Furthermore, for the planes with bigger $c$ index the distance $d$ is obviously shortened after implantation while $d$ does not change much for those with bigger $a$ and $b$ indexes (see table 4). The decrease of $c$ axis implies that Cu–O planes in the orthophase structure are closer to the Cu–O tetrahedron, thus enhancing their interaction [8]. This may be one of the reasons that proton irradiation can raise the transition temperature of superconducting film YBaCuO.

Table 2
Relative intensities of X-ray diffraction peaks and $d$ values for the main crystal planes of YBaCuO film with YSZ substrate before and after hydrogen implantation.

| Crystal plane ($hkl$) | Non-implant | | Implant | |
|---|---|---|---|---|
| | $d$ | $I/I_0$ | $d$ | $I/I_0$ |
| 002 | 5.819 | 9.3 | 5.793 | 4.9 |
| 003 | 3.887 | 17.5 | 3.870 | 9.9 |
| 100 | 3.816 | 12.9 | 3.808 | 6.5 |
| 012 | 3.235 | 6.0 | 3.188 | 4.9 |
| 102 | 3.195 | 7.0 | 3.128 | 3.5 |
| 103 | 2.720 | 100 | 2.715 | 100 |
| 110 | 2.720 | 100 | 2.715 | 100 |
| 005 | 2.334 | 7.5 | 2.329 | 20.8 |
| 113 | 2.230 | 11.0 | 2.225 | 11.8 |
| 020 | 1.942 | 13.8 | 1.942 | 32.4 |
| 006 | 1.942 | 13.8 | 1.942 | 32.4 |
| 200 | 1.909 | 43.9 | 1.908 | 19.9 |
| 016 | 1.740 | 5.9 | 1.733 | 3.4 |
| 023 | 1.740 | 5.9 | 1.733 | 3.4 |
| 123 | 1.580 | 14.5 | 1.580 | 12.2 |
| 116 | 1.580 | 14.5 | 1.580 | 12.2 |
| 213 | 1.568 | 16.2 | 1.566 | 8.6 |

Table 3
Comparison of relative intensities for three pairs of crystal planes of YBaCuO films before and after implantation.

| Crystal planes | Before | After |
|---|---|---|
| (012) and (102) | 6.0: 7.0 | 4.9: 3.5 |
| (020) and (200) | 13.8:43.9 | 32.4:19.9 |
| (123) and (213) | 14.5:16.2 | 12.2: 8.6 |

Table 4
Variation of $c$ axes for three crystal planes of the YBaCuO film before and after proton implantation.

| Planes | Before | After |
|---|---|---|
| 002 | 11.638 | 11.590 |
| 003 | 11.661 | 11.610 |
| 005 | 11.670 | 11.645 |





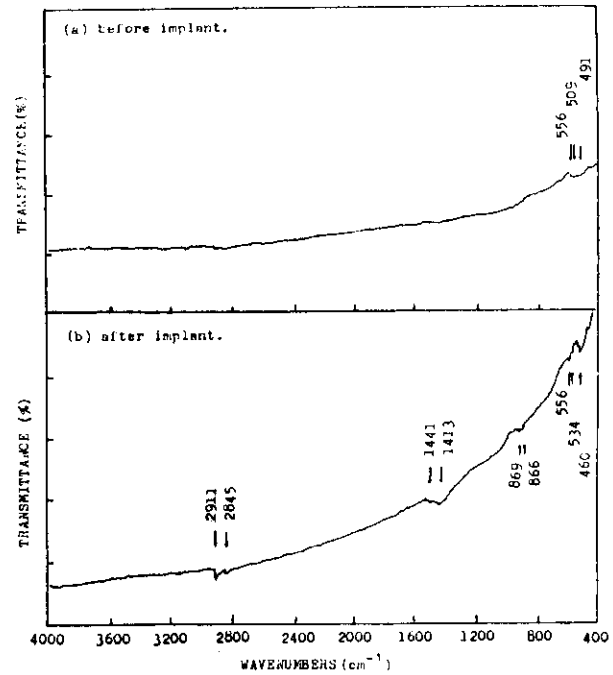


Fig. 4. Infrared absorption spectra of YBaCuO film with YSZ substrate: (a) before implantation, (b) after implantation.

Infrared absorption spectroscopy is one of the techniques useful for the study of the secondary and tertiary structures in solids: figs. 4a and 4b illustrate typical infrared spectra of the superconducting YBaCuO film with YSZ substrate before and after hydrogen implantation respectively.

In the IR spectrum of non-implanted YBaCuO film only three bands at 556, 509 and 491 $cm^{-1}$ have been observed at the low end of the spectrum, and they are associated with a metal–oxide (M–O) bond (fig. 4a). After hydrogen implantation these bands still exist but the intensities and positions are changed as shown in fig. 4b, for instance, 556, 534 and 460 $cm^{-1}$.

In the spectrum of the irradiated YBaCuO film there appear new bands at the positions of 2911, 2845, 1441, 1413 as well as 869 and 866 $cm^{-1}$. It is estimated that the new bands at the 2911 and 2845 $cm^{-1}$ come from vibrations of Cu–H bonds located

at the Cu–O chain and in the center of the Cu–O tetrahedron respectively. 1441 and 1413 $cm^{-1}$ bands are the higher order of their corresponding vibrations. At present it is not clear whether the bands at 869 and 866 $cm^{-1}$ are due to the Cu–H bond at the environment different from the above or due to other localized vibrations characteristic of new conformation of the M–O segment by energy deposition with proton implantation. However, it is quite certain that none of the above-mentioned bands is attributed to the H–O group at the surface water of the sample since the IR absorption peaks for the surface water are positioned at 3400, 1640 and 650 $cm^{-1}$.

## 5. Conclusion and discussion

From the above study we may draw the following conclusions:

(1) Hydrogen implantation can modify superconductivity of YBaCuO films and this modification is closely related to the properties and structures of the film-supporting materials. With the substrate of YSZ single crystal the zero resistance temperature $T_{c0}$ can be greatly increased and the electric properties above the transition temperature are improved.

(2) The energetic protons can change the microstructure of the YBaCuO superconducting film. The distance $d$ for the crystal planes with bigger $c$ index is obviously shortened after implantation. This may enhance the interaction between them and be beneficial to the improvement of superconductivity of YBaCuO film.

(3) The formation of Cu–H bonds by proton implantation does not induce hydrolysis of ceramic oxide superconductor. On the contrary, it may stabilize electric properties of the superconducting YBaCuO materials [7]. The proton-irradiated film samples which have experienced various kinds of measurements and stored at atmospheric condition for three months keep well-superconducting.

It is known that ion implantation can not only dope impurities and induce radiation damage in solid materials, but also play a role analogous to high temperature or pressure by energy deposition in the solid film, which can stabilize the film structures not normally obtained at the substrate [9]. These processes would influence composition, structure and electronic properties of the film. However, it is hard to say at present, whether the enhancement of $T_{c0}$ and the improvement of electric properties for H-implanted YBaCuO film with YSZ substrate come from microstructural change or from Cu–H bond formation or both. The mechanism for proton beam modification of superconducting film remains to be studied further. Our experimental results demonstrate that hydrogen implantation affects superconductivity and microstructures of YBaCuO films, which in turn are related to the supporting materials.

## Acknowledgement

Acknowledgement is made to Professors P.H. Wu and D. Feng for their support of our work.

## References

[1] W. Büchel and B. Stritzker, Application of ion beams to metals, eds. S.T. Picraux et al. (Plenum, New York, 1974).
[2] O. Meyer, New uses of ion accelerators, ed. J.D. Ziegler (Plenum, New York, 1985) p. 323.
[3] G.H. Wang, Acta Phys. Sin. 33 (1984) 1434.
[4] J.G. Bednorz and K.A. Müller, Z. Phys. B 64 (1986) 189.
[5] M.K. Wu, J.R. Ashburn, C.J. Torng, P.H. Hor, R.L. Meng, L. Gao, Z.J. Huang, Y.Q. Wang and C.W. Chu, Phys. Rev. Lett. 58 (1987) 908;
Z.X. Zhao, L.Q. Chen, Q.S. Yang, Y.Z. Huang, G.H. Chen, R.M. Tung, G.R. Liu, C.G. Gui, L. Chen, L.H. Wang, S.Q. Guo, S.Q. Guo, S.L. Li and J.Q. Bi, Kuxue Tongbao 32 (1987) 661.
[6] R.B. Laibowitz, R.H. Koch, P. Chaudhari and R.J. Gambino, Phys. Rev. Lett., to be published.
[7] G.H. Wang, J. Chen, G.Q. Dang and C.L. Lou, Phys. Lett. A 131 (1988), to be published.
[8] S. Massidda, J. Yu, A.J. Freeman and D.D. Koelling, Phys. Lett. A 122 (1987) 198.
[9] J.M. Harper, J.J. Cuomo, R.J. Gambino and H.R. Kaufman, Ion bombardment modification of surfaces, eds. O. Auciello and R. Kelly (Elsevier, Amsterdam, 1984) p. 127.